

surements, the metallic intercalates ($x = 1.85, 2$) appear to be mixed-valency compounds. The impurity band ($\text{Sn } 5s^2$) probably consists of a few delocalized states near the Fermi level, whereas the states near the bottom of the band are still under the localizing influence of the parent $[\text{CoCp}_2]^+$ potential.

Finally, the neutral cobaltocene species must contribute HOMO $\text{Co}(3d\pi^*)$ states in the band gap overlapping with the main $\text{Sn } 5s^2$ impurity band (Figure 8).

Conclusion

The intercalation of cobaltocene into the single crystals of the layered tin dichalcogenides $\text{SnS}_{2-x}\text{Se}_x$ has presented the opportunity to study the electronic structure changes taking place by using photoelectron spectroscopy. For this work it was essential to prepare single crystals, which can be cleaved in UHV to give clean, undisturbed surfaces. The systematic variation of the sulfur and selenium content of these materials has produced an interesting variation in physical properties through the intercalate series.

The XPS core-level studies have shown that both the tin and cobalt species exhibit mixed oxidation states throughout the series. This observation has been taken as evidence that electron transfer is occurring between the guest and host entities upon intercalation. Intercalation of other guest molecules such as ferrocene (FeCp_2) and chromocene (CrCp_2) into the SnS_2 host has previously been attempted.¹¹ The lack of success in the disulfide case has not been

followed up in the selenium-containing hosts. However, attempts at intercalation of these guest molecules could be worthwhile, since, if successful, this would test the hypothesis that ferrocene (less reducing than cobaltocene) would give less extensive electron transfer to the tin sites, while chromocene (more reducing than cobaltocene) would give a greater degree of electron transfer. The intercalation of the $\text{Co}(\text{C}_5\text{Me}_5)_2$ molecule into the $\text{SnS}_{2-x}\text{Se}_x$ hosts might present a possibility of investigating the nature of the postulated nucleophilic attack on the guest molecule. However, in the SnS_2 instance, it is not possible to intercalate the $\text{Co}(\text{C}_5\text{Me}_5)_2$ molecule.¹¹

The valence-band study using UPS has demonstrated that the electron transfer has created new states in the band gap of the intercalates. Increasing the selenium content of the intercalates results in a transition from semiconducting to metallic behavior. The polarizability of the medium has been postulated as the crucial factor determining the nature of the states formed in the band gap upon intercalation.

The results of PES show clearly that the host properties have a great influence on the nature of the intercalated guest species and the overall electronic structure of these intercalated materials. Recent observations of superconductivity in these metallic intercalates²⁶ has given impetus to further work, which will concentrate on other physical measurements and the possibility of intercalating other guest molecules into these layered structures.

Contribution from the Departments of Chemistry, University Center at Binghamton, State University of New York, P.O. Box 6000, Binghamton, New York 13902-6000, and University of Southern California, Los Angeles, California 90089

Photophysical Studies of $\text{W}(\text{CO})_5\text{L}$ Complexes. Multiple-State Luminescence of $\text{W}(\text{CO})_5(4\text{-cyanopyridine})$ in Fluid and Glassy Solutions

Kathleen A. Rawlins,[†] Alistair J. Lees,^{*,†} and Arthur W. Adamson[‡]

Received February 14, 1990

Electronic absorption spectra, luminescence spectra, excitation data, and luminescence lifetimes have been recorded from $\text{W}(\text{CO})_5(4\text{-CNpy})$ and $\text{W}(\text{CO})_5(\text{pip})(4\text{-CNpy})$ ($4\text{-CNpy} = 4\text{-cyanopyridine}$; $\text{pip} = \text{piperidine}$) complexes in methylcyclohexane solutions at 210–313 K and in EPA glasses at 77 K. The results illustrate that $\text{W}(\text{CO})_5(4\text{-CNpy})$ is a multiple-state emitter displaying dual emission bands at any of the measured temperatures; the emitting levels are assigned to metal to ligand charge-transfer (MLCT) excited states that are predominantly of triplet character. In fluid solution the two ³MLCT emitting levels establish a thermal equilibrium and the luminescence data obtained from temperatures between 210 and 313 K can be fitted to a modified Boltzmann model yielding an energy separation between the participating states of 990 (± 50) cm^{-1} . In a frozen glass the two radiative ³MLCT excited states are no longer thermally equilibrated, as evidenced by their different emission lifetime values and by an excitation wavelength dependence in the emission spectra. Luminescence spectra and lifetimes have also been observed from $\text{W}(\text{CO})_5(\text{pip})$ at low temperature, and its emitting level is assigned to a ligand field (LF) state of predominantly triplet character. No evidence has been obtained for a ³LF radiative route in $\text{W}(\text{CO})_5(4\text{-CNpy})$, even at 77 K; this result, taken in conjunction with prior photochemical studies, indicates that although the LF levels are effectively populated on near-UV light excitation, they undergo very efficient radiationless deactivation, including conversion to the emitting ³MLCT excited-state manifold.

Introduction

Photophysical studies of transition-metal organometallic complexes are essential in determining and characterizing their lowest lying electronically excited states. In several metal complex systems, luminescence techniques have been used most successfully as spectroscopic probes to provide valuable insight into the nature of their often intricate excited-state levels and deactivation pathways.¹

The $\text{W}(\text{CO})_5\text{L}$ ($\text{L} = \text{a substituted pyridine}$) system is of special significance because these complexes were the first 6 metal carbonyls observed to luminescence in frozen glasses² and in fluid solution.³ Indeed, their electronically excited states are among the longest lived determined to date for group 6 metal carbonyl systems, exhibiting emission lifetimes of over 400 ns in room-

temperature solution.^{1,3b} Despite this knowledge, a number of aspects concerning their photophysical properties remain to be understood. Specifically, although these molecules are known to possess two lowest energy metal to ligand charge-transfer (MLCT) transitions and a proximate ligand field (LF) transition,⁴ the exact role of these states in the photophysical deactivation mechanism is not clear. The earlier published photophysical work^{3b} clearly implicated the presence of two close-lying MLCT excited levels

- (1) Lees, A. J. *Chem. Rev.* **1987**, *87*, 711 and references therein.
- (2) (a) Wrighton, M.; Hammond, G. S.; Gray, H. B. *J. Am. Chem. Soc.* **1971**, *93*, 4336. (b) Wrighton, M.; Hammond, G. S.; Gray, H. B. *Inorg. Chem.* **1972**, *11*, 3122. (c) Wrighton, M.; Hammond, G. S.; Gray, H. B. *Mol. Photochem.* **1973**, *5*, 179. (d) Wrighton, M. S.; Abrahamson, H. B.; Morse, D. L. *J. Am. Chem. Soc.* **1976**, *98*, 4105.
- (3) (a) Lees, A. J.; Adamson, A. W. *J. Am. Chem. Soc.* **1980**, *102*, 6874. (b) Lees, A. J.; Adamson, A. W. *J. Am. Chem. Soc.* **1982**, *104*, 3804.
- (4) Geoffroy, G. L.; Wrighton, M. S. *Organometallic Photochemistry*; Academic: New York, 1979 (and references therein).

[†]SUNY.
[‡]USC.

in the deactivation processes, and yet, the nature of the non-radiative interconversion mechanisms is not fully characterized. In addition, while the $W(CO)_5L$ photochemistry has been extensively studied, the manner in which the photochemically active states participate in the photophysical deactivation mechanism still needs to be completely rationalized.

With these objectives in mind, we have undertaken a detailed investigation of the luminescence from $W(CO)_5(4-CNpy)$ ($4-CNpy = 4\text{-cyanopyridine}$) over a range of temperatures and solution environments. The results obtained not only indicate that the $W(CO)_5(4-CNpy)$ complex is a multiple-state emitter in both glassy and fluid solutions but also help us provide a description on the nature of the dynamic processes that exist between the participating emitting excited states. The important role of the photochemically active levels is also assessed by a comparison with the photophysical properties of $W(CO)_5(pip)$ ($pip = piperidine$).

Experimental Section

Materials. Tungsten hexacarbonyl was obtained from Strem Chemical Co. and purified by sublimation. The $4-CNpy$ ligand was obtained from Aldrich Chemical Co. and purified by sublimation. Piperidine (pip) was also obtained from Aldrich, and it was purified by distillation immediately prior to use. Methylcyclohexane used was high-purity Photrex grade received from Baker Chemical Co. EPA (ether-isopentane-ethanol, 5:5:2 by volume) comprised rigorously dried solvent components that had been individually distilled repeatedly to remove emitting impurities. Neutral alumina (80–200 mesh) was used for chromatographic purifications as received from Fisher Scientific Co. Nitrogen used for purging samples had been dried and deoxygenated as previously described.⁵

Synthesis. The $W(CO)_5(4-CNpy)$ and $W(CO)_5(pip)$ complexes were prepared photochemically via the corresponding $W(CO)_5(THF)$ ($THF = \text{tetrahydrofuran}$) derivative, according to a procedure reported earlier.^{3b,6} Both compounds were purified by column chromatography on alumina. Infrared and UV-visible spectra recorded from the compounds agreed well with the literature.^{2d,3b}

Spectroscopic Measurements. Infrared spectra were obtained from the complexes as chloroform solutions with a NaCl cell of 1-mm path length, and the data were recorded on a Perkin-Elmer Model 283B spectrometer. UV-visible spectra were recorded on either a Perkin-Elmer Model 559 spectrometer (for glass studies) or a Hewlett-Packard Model 8450A diode-array spectrometer (for solution studies), and the reported maxima are accurate to ± 2 nm.

Luminescence and excitation spectra were obtained on a SLM Instruments Model 8000/8000S dual-monochromator spectrometer, which incorporates a photomultiplier-based photon-counting detector. A red-sensitive Hamamatsu R928 photomultiplier tube was used in these measurements. For each complex the resultant emission band maxima were found to be reproducible to ± 4 nm. Luminescence excitation spectra were determined from samples that were optically dilute ($A < 0.1$) throughout the spectral region scanned and were corrected for wavelength variations in exciting-lamp intensity. In all these emission experiments the sample solutions were filtered through 0.22- μm Millipore filters and then deoxygenated by N_2 -purging for 15 min prior to taking measurements. Readings were taken from solutions contained in a 1 cm square quartz cell. IR and UV-visible spectra were checked before and after irradiation to monitor possible sample degradation. For studies between 268 and 313 K, the solution temperatures were controlled to ± 0.1 K by circulating a thermostated ethylene glycol-water mixture through a jacketed cell holder placed in the emission apparatus.

Absorption and luminescence measurements at temperatures below 268 K were performed with an Oxford Instruments DN1704K liquid- N_2 cooled variable-temperature cryostat fitted with synthetic sapphire inner windows and quartz outer windows. Samples were contained in a fused-quartz 1 cm path length square cell and rigorously deaerated by successive freeze-pump-thaw cycles. The temperature was maintained to ± 0.2 K with an Oxford Instruments Model 3120 controller.

Luminescence lifetimes were recorded on a PRA System 3000 time-correlated pulsed single-photon-counting spectrometer.⁷ Samples were excited with light from a N_2 -filled PRA Model 510 flash lamp transmitted through an Instruments SA Inc. H-10 monochromator. Emission was detected at 90° via a second Instruments SA Inc. H-10 monochromator onto a thermoelectrically cooled red-sensitive Hamamatsu R955

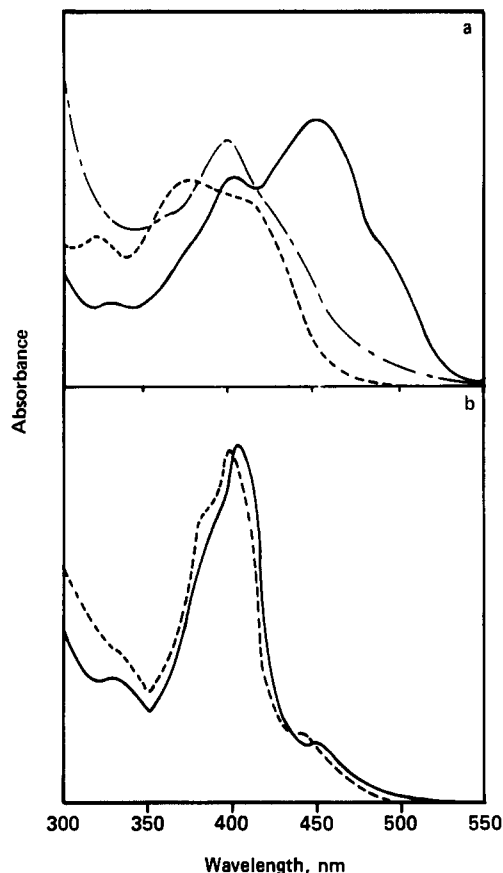


Figure 1. Electronic absorption spectra of (a) $W(CO)_5(4-CNpy)$ and (b) $W(CO)_5(pip)$ in (—) methylcyclohexane solution at 296 K and (---) EPA glass at 77 K. The absorption spectrum of $W(CO)_5(4-CNpy)$ in EPA at 296 K (---) is also shown.

photomultiplier tube. The resulting photon counts were stored on a Tracor Northern Model 7200 microprocessor-based multichannel analyzer. The instrument response function was subsequently deconvoluted from the luminescence data to obtain an undisturbed decay that was fitted by using an iterative least-squares procedure on an IBM-PC. Reported lifetimes were reproducible to the quoted errors over at least three readings.

Results

Figure 1 depicts electronic absorption spectra observed from $W(CO)_5(4-CNpy)$ in a methylcyclohexane solution at 296 K and in EPA solution at both 296 and 77 K. These spectra illustrate that the lowest energy absorptions of $W(CO)_5(4-CNpy)$ blue-shift substantially on moving from the nonpolar methylcyclohexane solution to the polar EPA solution. In addition, there is a further blue shift when the EPA solution is cooled to a glass. Analogous spectra of $W(CO)_5(pip)$ are also included for comparison, and they indicate that the lowest lying absorption bands are relatively unshifted when the solution forms a glass. Molar absorptivities for these compounds have been previously reported in the literature as $8680 \text{ M}^{-1} \text{ cm}^{-1}$ (at 454 nm) for $W(CO)_5(4-CNpy)$ in methylcyclohexane and $3960 \text{ M}^{-1} \text{ cm}^{-1}$ (at 407 nm) for $W(CO)_5(pip)$ in isoctane.^{2d,3b}

Figure 2 shows luminescence spectra recorded from $W(CO)_5(4-CNpy)$ in deoxygenated methylcyclohexane solution at 296 K. Two emission bands are clearly displayed centered at 545 and 613 nm. In EPA solution at 296 K, these bands are observed at 492 nm and as a broad feature centered between 600 and 650 nm; these emission bands are of weak intensity and are apparently quenched significantly by the polar medium. Importantly, the dual-luminescence spectral distribution of $W(CO)_5(4-CNpy)$ in solution was not affected by variations in excitation wavelength over the 275–425-nm region. Indeed, this was observed to be the case at any temperature above the methylcyclohexane glass thawing point (> 210 K), where the solution is completely fluid. No luminescence was detected from $W(CO)_5(pip)$ at 296 K in

(5) Schadt, M. J.; Lees, A. J. *Inorg. Chem.* **1986**, *25*, 672.

(6) Kolodziej, R. M.; Lees, A. J. *Organometallics* **1986**, *5*, 450.

(7) O'Connor, D. V.; Phillips, D. *Time-Correlated Single Photon Counting*; Academic: London, 1984.

Table I. Electronic Absorption, Luminescence, and Excitation Maxima and Luminescence Lifetimes for $W(CO)_5(4-CNpy)$ and $W(CO)_5(pip)$ in Methylcyclohexane (MCH) and EPA Solutions at 296 and 77 K^a

complex	environment	abs λ_{max} , nm	exc λ_{max} , nm	luminescence	
				λ_{max} , nm	τ_e , μs
$W(CO)_5(4-CNpy)$	MCH, 296 K	335, 371 (sh), 404, 454, 495 (sh)	371 (sh), 405, 460, 505 (sh) 371 (sh), 405, 460, 505 (sh)	545 613	0.292 0.292
	EPA, 296 K	365 (sh), 402, 436	<i>b</i> <i>b</i>	492 600–650 (br)	<i>b</i> <i>b</i>
	EPA, 77 K	322, 381, 423	343, 367, 403 371, 397, 440	489 593	11.4 20.1
$W(CO)_5(pip)$	MCH, 296 K	384 (sh), 405, 450 (sh)		<i>c</i>	
	EPA, 77 K	378 (sh), 400, 441 (sh)	373, 397, 445	532	4.7

^aLuminescence spectra recorded following excitation at 400 nm; lifetimes and excitation data obtained at the corresponding luminescence maxima; sh = shoulder; br = broad. ^bLuminescence only weakly observed, and excitation data and lifetime not obtained. ^cNo luminescence observed.

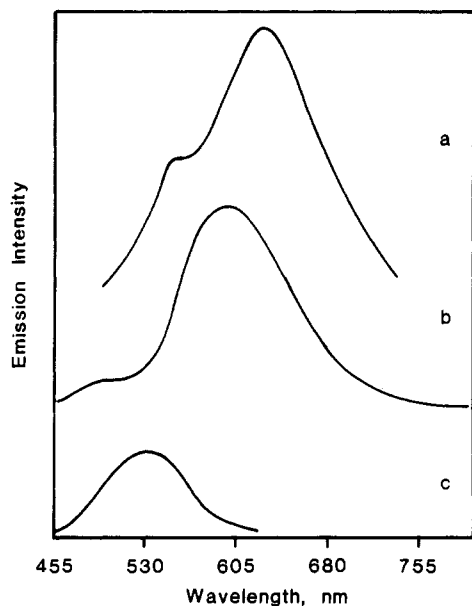


Figure 2. Luminescence spectra of (a) $W(CO)_5(4-CNpy)$ in methylcyclohexane solution at 296 K, (b) $W(CO)_5(4-CNpy)$ in an EPA glass at 77 K, and (c) $W(CO)_5(pip)$ in an EPA glass at 77 K. Excitation wavelength is 400 nm in each case.

either deoxygenated benzene, methylcyclohexane or EPA.

When the $W(CO)_5(4-CNpy)$ complex is cooled and forms a frozen glass at 77 K, the luminescence intensities of both bands increase by approximately 100-fold over that observed from room-temperature solutions. Luminescence spectra obtained from $W(CO)_5(4-CNpy)$ in an EPA glass at 77 K are illustrated in Figure 2; two emission bands are again observed in the spectrum at 489 and 593 nm. Significantly, the low-temperature luminescence spectral distribution exhibits a substantial excitation wavelength dependence whereby the intensity of the upper energy band increases relative to the lower energy band as the exciting wavelengths become shorter from 400 to 300 nm. Moreover, in an EPA glass at 77 K, luminescence is now readily detected from $W(CO)_5(pip)$ as a single band feature centered at 532 nm (see Figure 2). Notably, though, the intensities of these $W(CO)_5(pip)$ luminescence spectra are at least 20-fold less than the corresponding low-temperature $W(CO)_5(4-CNpy)$ spectra.

Figure 3 illustrates an excitation spectrum representative of those recorded from $W(CO)_5(4-CNpy)$ in methylcyclohexane solution at 296 K. Importantly, the excitation spectral distribution observed here did not change on varying the wavelength at which the emission is monitored throughout the $W(CO)_5(4-CNpy)$ dual-luminescence band envelope. On the other hand, excitation spectra recorded from $W(CO)_5(4-CNpy)$ at low temperature do exhibit a substantial dependence on the monitoring emission wavelength; excitation results obtained while light at the two emission maxima was detected are depicted in Figure 3. The excitation spectrum of $W(CO)_5(pip)$ in EPA at 77 K has also been obtained and found not to vary with changes in the monitoring

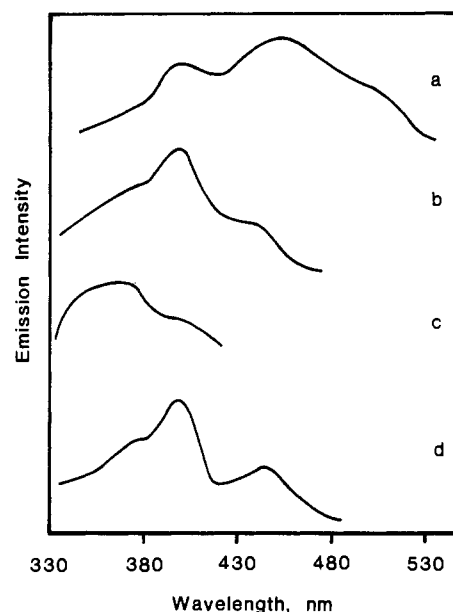


Figure 3. Excitation spectra of (a) $W(CO)_5(4-CNpy)$ in methylcyclohexane solution at 296 K ($\lambda_{em} = 600$ nm), (b and c) $W(CO)_5(4-CNpy)$ in an EPA glass at 77 K ($\lambda_{em} = 600$ and 500 nm, respectively), and (d) $W(CO)_5(pip)$ in an EPA glass at 77 K ($\lambda_{em} = 530$ nm).

wavelength; a representative spectrum is also shown in Figure 3.

Luminescence lifetimes have been measured at both room and low temperatures. For $W(CO)_5(4-CNpy)$ in 296 K methylcyclohexane, the lifetimes obtained from the upper and lower emission bands are the same, within the experimental uncertainty, at 292 (± 15) ns. In contrast, the observed lifetimes in EPA at 77 K of these two emission bands are not equal, being 11.4 (± 1.1) μs for the upper emission and 20.1 (± 2.0) μs for the lower emission. The luminescence lifetime of $W(CO)_5(pip)$ in 77 K EPA was determined to be 4.7 (± 0.5) μs .

Table I summarizes the recorded absorption, emission, and excitation maxima and emission lifetimes for both complexes in various solution environments.

Figure 4 depicts changes observed on the luminescence spectrum of $W(CO)_5(4-CNpy)$ in methylcyclohexane solution as the temperature is varied between 268 and 313 K. When the temperature is raised, the emission spectral distribution changes significantly with the higher energy band becoming relatively more intense compared to the lower energy band. These spectra were each recorded following excitation at 400 nm; at any one of the individual temperatures, however, the spectra were not found to vary with changes in the exciting wavelength.

Discussion

Excited-State Assignments. Previously, the electronic structures of $W(CO)_5L$ complexes have been investigated in considerable detail.^{2,3,8} Several studies concerning the electronic absorption,

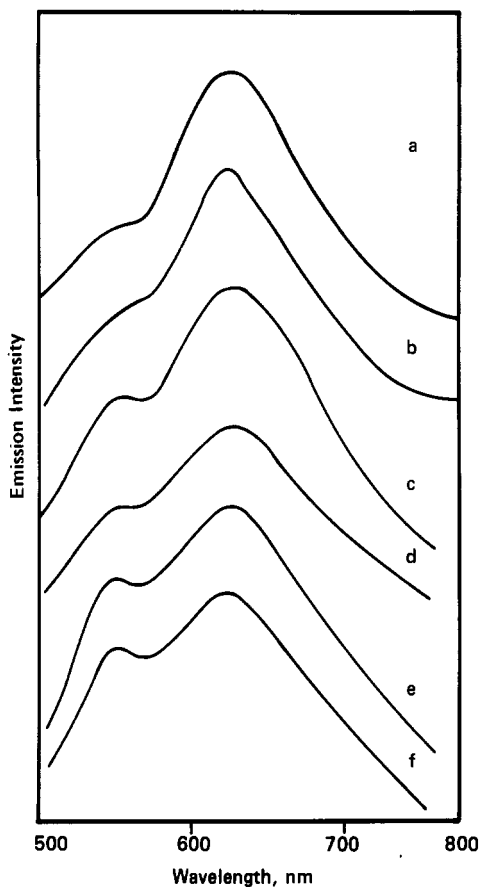


Figure 4. Temperature dependence of the uncorrected luminescence spectra of $W(CO)_5(4-CNpy)$ in methylcyclohexane solution. The temperatures are (a) 268 K, (b) 278 K, (c) 288 K, (d) 296 K, (e) 303 K, and (f) 313 K. All spectra have been normalized, and the excitation wavelength is 400 nm in each case.

photochemical reactivity, and luminescence properties of these molecules have demonstrated that the $W(CO)_5L$ system comprises lowest lying MLCT and LF states, their exact order depending on the nature of the ligand L. The $W(CO)_5L$ complexes may be viewed in C_{4v} symmetry, and simple one-electron orbital level representations for the derivatives under study are portrayed in Figure 5. In this description the lowest lying excited levels of the $W(CO)_5(pip)$ complex are of LF character and these are associated with efficient ($\phi = 0.58$) ligand photosubstitution chemistry.^{2d} On the other hand, the $W(CO)_5(4-CNpy)$ complex exhibits two lowest energy $(W)d\pi \rightarrow \pi^*(4-CNpy)$ MLCT levels and much reduced ($\phi = 0.02$) photoreactivity.^{2d,3b} The absorption and luminescence data obtained in the present study can, to a large extent, be rationalized in terms of the excited states deriving from this simple orbital model. For convenience, the two lowest lying $(W)d\pi \rightarrow \pi^*(4-CNpy)$ transitions will subsequently be referred to as the MLCT(e) and MLCT(b_2) states, according to their respective orbital symmetry designations.

UV-visible spectra observed from the $W(CO)_5L$ complexes (see Figure 1) support the LF/MLCT description. The $W(CO)_5(pip)$

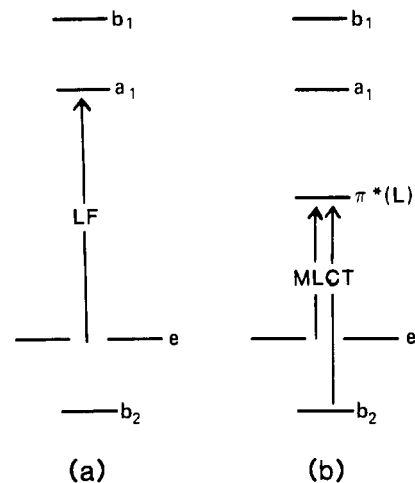


Figure 5. One-electron orbital schemes for C_{4v} complexes: (a) $W(CO)_5(pip)$; (b) $W(CO)_5(4-CNpy)$.

derivative exhibits only LF transitions, its lowest "singlet" state at ~ 405 nm and the corresponding "triplet" level at ~ 450 nm.⁹ These bands are hardly moved upon cooling the solution through the glass transition point, consistent with their metal-centered characters. In comparison, the 296 K spectrum of the $W(CO)_5(4-CNpy)$ complex not only exhibits the features of these LF absorptions but is dominated by lowest lying MLCT(b_2) and MLCT(e) transitions centered at 454 and ~ 495 (sh) nm, respectively. When the nonpolar methylcyclohexane solution is replaced by a polar EPA solution, these MLCT absorptions blue-shift substantially and overlap with the lowest lying LF absorptions. When the EPA solution is cooled and forms a frozen glass, there is an additional blue shift in the MLCT absorption envelope. These effects are understood to be caused by alterations in the local solvent environment and, specifically, changes in the nature of the solute-solvent dipolar interaction in polar and nonpolar solutions and on freezing.¹⁰

Luminescence spectra obtained from the $W(CO)_5L$ complexes (see Figure 2) also support a LF/MLCT model. For $W(CO)_5(pip)$, luminescence was only observable at low temperature in a rigid environment, where the photosubstitution efficiency of the LF manifold is diminished. Even so, the emission observed from this complex was relatively weak. In contrast, the $W(CO)_5(4-CNpy)$ complex gives rise to two much more intense luminescence bands at either low or room temperature and these are attributed to the lowest lying ${}^3MLCT(b_2)$ and ${}^3MLCT(e)$ levels. Moreover, these $W(CO)_5(4-CNpy)$ emissions are distinct in their wavelength positions and lifetimes from those of the $W(CO)_5(pip)$ data, and no experimental evidence has been found to invoke a radiative 3LF state in the former complex, at either 296 or 77 K. However, as the emission intensity was noted to be so much weaker from the $W(CO)_5(pip)$ complex, a reasonable explanation may be that any 3LF emission in $W(CO)_5(4-CNpy)$ at 77 K is simply overwhelmed by the more intense 3MLCT bands. Further evidence for the 3MLCT assignment is gathered from the significant blue spectral shift in the emission band that is noted when the methylcyclohexane solution is replaced by EPA and, additionally, when the EPA solution is cooled to form a glass. The majority of the change that occurs here is reflected in the movement to shorter wavelength of the lowest energy ${}^3MLCT(e)$ emission band. The blue shift observed on cooling the EPA to 77 K is one that has been recognized for several other luminescent organometallic compounds exhibiting 3MLCT excited states.^{1,11,12} This effect

- (8) (a) Darensbourg, D. J.; Brown, T. L. *Inorg. Chem.* **1968**, *7*, 959. (b) Dahlgren, R. M.; Zink, J. I. *Inorg. Chem.* **1977**, *16*, 3154. (c) Dahlgren, R. M.; Zink, J. I. *J. Am. Chem. Soc.* **1979**, *101*, 1448. (d) Frazier, C. C.; Kisch, H. *Inorg. Chem.* **1978**, *17*, 2736. (e) McHugh, T. M.; Narayanaswamy, R.; Rest, A. J.; Salisbury, K. *J. Chem. Soc., Chem. Commun.* **1979**, 208. (f) Boxhoorn, G.; Oskam, A.; Gibson, E. P.; Narayanaswamy, R.; Rest, A. J. *Inorg. Chem.* **1981**, *20*, 783. (g) Boxhoorn, G.; Schoemaker, G. C.; Stufkens, D. J.; Oskam, A.; Rest, A. J.; Darensbourg, D. J. *Inorg. Chem.* **1980**, *19*, 3455. (h) Tutt, L.; Tannor, D.; Heller, E. J.; Zink, J. I. *Inorg. Chem.* **1982**, *21*, 3858. (i) Tutt, L.; Tannor, D.; Schindler, J.; Heller, E. J.; Zink, J. I. *J. Phys. Chem.* **1983**, *87*, 3017. (j) Dillinger, R.; Gliemann, G. *Chem. Phys. Lett.* **1985**, *122*, 66. (k) Dillinger, R.; Gliemann, G. *Z. Naturforsch.* **1986**, *41*, 1071.

- (9) The large degree of spin-orbit coupling in these tungsten carbonyl complexes precludes "pure" singlet and triplet descriptions.
 (10) (a) Manuta, D. M.; Lees, A. J. *Inorg. Chem.* **1986**, *25*, 3212. (b) Zulu, M. M.; Lees, A. J. *Inorg. Chem.* **1988**, *27*, 3325.
 (11) (a) Wrighton, M.; Morse, D. L. *J. Am. Chem. Soc.* **1974**, *96*, 998. (b) Giordano, P. J.; Fredericks, S. M.; Wrighton, M. S.; Morse, D. L. *J. Am. Chem. Soc.* **1978**, *100*, 2257.

has been referred to as "luminescence rigidochromism",¹¹ and is believed to be a type of solvent effect relating to the substantial changes that take place in the local solvent environment accompanying a reorientation of the solvent dipoles on passing through the glass transition point.

Finally, the excitation spectra of $W(CO)_5(4-CNpy)$ and $W(CO)_5(pip)$ can be understood in terms of the ${}^3LF/{}^3MLCT(b_2)/{}^3MLCT(e)$ model. The observed spectrum from $W(CO)_5(4-CNpy)$ in methylcyclohexane at 296 K (see Figure 3a) depicts fairly good congruence with the absorption data (see Figure 1a), and thus, it fits with the notion of two low-energy 3MLCT emitting levels. This excitation spectrum also matches the absorption spectrum in the higher energy LF region, indicating that these levels effectively deactivate to the ${}^3MLCT(b_2)/{}^3MLCT(e)$ manifold. In low-temperature EPA, though, the excitation spectra of $W(CO)_5(4-CNpy)$ reveal significant wavelength effects (see Figure 3b,c), indicating that the ${}^3MLCT(b_2)$ and ${}^3MLCT(e)$ levels radiate independently. Indeed, the low-temperature absorption spectrum (see Figure 1a) is in good agreement with the sum of these two excitation spectra. The excitation spectrum of $W(CO)_5(pip)$ in EPA at 77 K is also congruent with the low-temperature absorption result (see Figures 1b and 3d), and this identifies the origin of the emission in this complex to the ${}^1LF/{}^3LF$ states.

Excited-State Dynamics. In recent years a number of multiple-state luminescence systems have been established, but most cases involve multiple emission at low temperature.^{1,13-16} The $W(CO)_5(4-CNpy)$ molecule is particularly significant because the dual-luminescence spectrum is observed from the complex in fluid solution and the participating emitting levels are relatively long-lived. Hence, the dynamic processes that exist between the excited states here are of importance.

Analysis of the luminescence data leads to the conclusion that the two emitting ${}^3MLCT(b_2)$ and ${}^3MLCT(e)$ states are in thermal equilibrium under room-temperature-solution conditions. This is because the observed luminescence spectra exhibit no excitation wavelength dependence and because the emission lifetimes of the participating 3MLCT states are found to be equivalent. Moreover, the obtained excitation spectrum of $W(CO)_5(4-CNpy)$ at room temperature is not affected by changes in the monitoring emission wavelength throughout the dual-luminescence band, consistent with a model involving two thermally equilibrated emitting levels. From data recorded just above the glass transition point, it can be inferred that the thermal equilibrium appears to exist at any temperature where the solution is still fluid. Contrastingly, the results obtained from the glassy solutions illustrate that the thermal equilibrium between the two 3MLCT emitting states does not exist when the solution is rigid. At 77 K the luminescence spectral distribution is observed to be dependent on the wavelength of the exciting light, the emission lifetimes of the participating 3MLCT

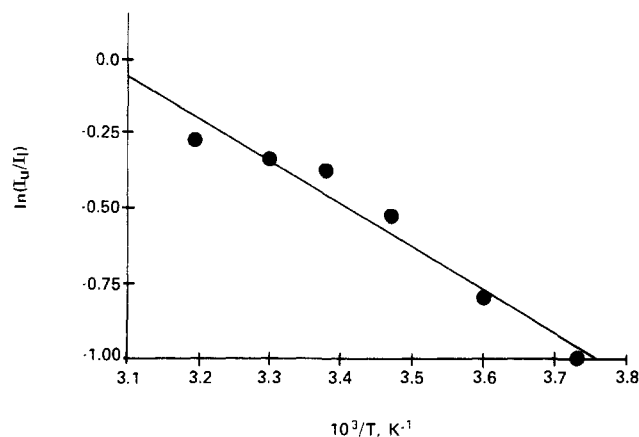


Figure 6. Plot of $\ln(I_u/I_l)$ vs $1/T$.

states are not equal, and the excitation spectra distribution depends on whether the emission is monitored at the lower or higher energy 3MLCT features.

In further developing a model to describe the 3MLCT dynamic processes, we recorded luminescence spectral data over a range of fluid-solution temperatures between 268 and 313 K (see Figure 4). These spectra lead us to suggest that there is a Boltzmann relationship between the ${}^3MLCT(b_2)$ and ${}^3MLCT(e)$ emitting levels. In adopting a Boltzmann model, we assume that the rate of interconversion between the two 3MLCT emitting levels is rapid compared to the rates of deactivation from these individual levels.¹⁷ Subsequently, the temperature dependence data of Figure 4 can be fitted to the modified Boltzmann expression shown in eq 1.^{12b,14b,15a,17} Here, I_u and I_l are the luminescence intensities of

$$\ln \frac{I_u}{I_l} = \left(\ln \frac{g_u k_u}{g_l k_l} \right) - \frac{\Delta E}{k_B T} \quad (1)$$

the upper (u) ${}^3MLCT(b_2)$ and lower (l) ${}^3MLCT(e)$ levels measured at 545 and 613 nm, respectively, k_u and k_l represent the radiative rate constants of these states, g is a degeneracy factor, ΔE denotes the energy gap between the emitting levels, k_B is the Boltzmann constant, and T is temperature. A least-squares analysis of the spectral results is shown in Figure 6 and yields $\Delta E = 990 (\pm 50) \text{ cm}^{-1}$. This energy gap is consistent with the rapid interconversion between the two 3MLCT states being just within a recognized equilibrium limit of $\sim 1000 \text{ cm}^{-1}$,¹⁷ and it agrees well with the few other reported multiply emissive systems that are understood to be thermally equilibrated in solution.^{12b,14b,15a,b} This result reflects the energy gap between the 0,0 levels of the two 3MLCT states and is notably much smaller than one would estimate ($\sim 2035 \text{ cm}^{-1}$) from the maxima of these solvent-broadened emission bands.

This photophysical study has clearly shown that the role of the ${}^1LF/{}^3LF$ levels in $W(CO)_5(4-CNpy)$ is essentially a nonradiative one whereby these states effectively deactivate to the emitting MLCT states. However, the wealth of photochemical information that already exists on $W(CO)_5L$ complexes strongly indicates that the LF levels are also responsible for the photochemistry^{2d,3b,4} and, indeed, recent time-dependent analyses of emission and preresonance Raman spectra of $W(CO)_5(py)$ ($py = \text{pyridine}$) complexes have confirmed that on LF excitation the most significant distortion that takes place in the excited state involves a lengthening of the W-N bond.^{8h,i} Thus, the photochemistry in these and related $W(CO)_5L$ compounds can be rationalized to the lowest energy LF transition which populates the $a_1(\sigma^*)$ orbital (see Figure 5); complexes such as $W(CO)_5(pip)$, which have absorbing LF levels but no lower lying MLCT states, will, therefore, undergo an efficient bond dissociation ($\phi = 0.58$)^{2d} whereas those such as $W(CO)_5(4-CNpy)$, in which there is effective deactivation to MLCT levels, will have much reduced ligand dissociation processes ($\phi = 0.02$).^{2d,3b} Furthermore, the current results illustrate that

- (12) (a) Salman, O. A.; Drickamer, H. G. *J. Chem. Phys.* **1982**, *77*, 3337. (b) Zulu, M. M.; Lees, A. J. *Inorg. Chem.* **1989**, *28*, 85. (c) Rawlins, K. A.; Lees, A. J. *Inorg. Chem.* **1989**, *28*, 2154. (d) Glezen, M. M.; Lees, A. J. *J. Am. Chem. Soc.* **1989**, *111*, 6602.
- (13) (a) For a review of literature appearing up to 1980 see: DeArmond, M. K.; Carlin, C. M. *Coord. Chem. Rev.* **1981**, *36*, 325. (b) Segers, D. P.; DeArmond, M. K.; Grutsch, P. A.; Kutal, C. *Inorg. Chem.* **1984**, *23*, 2874. (c) Blakley, R. L.; Myrick, M. L.; DeArmond, M. K. *J. Am. Chem. Soc.* **1986**, *108*, 7843.
- (14) (a) Rader, R. A.; McMillin, D. R.; Buckner, M. T.; Matthews, T. G.; Casadonte, D. J.; Lengel, R. K.; Whittaker, S. B.; Darmon, L. M.; Lytle, F. E. *J. Am. Chem. Soc.* **1981**, *103*, 5906. (b) Kirchhoff, J. R.; Gamache, R. E.; Blaskie, M. W.; Del Paggio, A. A.; Lengel, R. K.; McMillin, D. R. *Inorg. Chem.* **1983**, *22*, 2380. (c) Casadonte, D. J.; McMillin, D. R. *J. Am. Chem. Soc.* **1987**, *109*, 331.
- (15) (a) Watts, R. J.; Missimer, D. J. *J. Am. Chem. Soc.* **1978**, *100*, 5350. (b) Watts, R. J. *Inorg. Chem.* **1981**, *20*, 2302. (c) Sexton, D. A.; Ford, P. C.; Magde, D. J. *J. Phys. Chem.* **1983**, *87*, 197. (d) Nishizawa, M.; Suzuki, T. M.; Sprouse, S.; Watts, R. J.; Ford, P. C. *Inorg. Chem.* **1984**, *23*, 1837.
- (16) (a) Kirk, A. D.; Porter, G. B. *J. Phys. Chem.* **1980**, *84*, 887. (b) Breddels, P. A.; Berdowski, P. A. M.; Blasse, G. *J. Chem. Soc., Faraday Trans. 2* **1982**, *78*, 595. (c) Martin, M.; Krogh-Jespersen, M.-B.; Hsu, M.; Tewksbury, J.; Laurent, M.; Viswanath, K.; Patterson, H. *Inorg. Chem.* **1983**, *22*, 647. (d) Belsler, P.; von Zelewsky, A.; Juris, A.; Barigelletti, F.; Balzani, V. *Chem. Phys. Lett.* **1984**, *104*, 100.

(17) Kemp, T. J. *Prog. React. Kinet.* **1980**, *10*, 301.

the presence of an overlapping and intensely absorbing MLCT band in the $W(CO)_5(4-CNpy)$ complex is also an important factor in reducing the efficiency of LF population and, hence, 3LF photochemistry.

Acknowledgment. We gratefully acknowledge the donors of the Petroleum Research Fund, administered by the American Chemical Society, for support of this research. We also thank Mr. Zhikai Wang for assistance with the lifetime measurements.

Contribution from the Laboratoire de Chimie Théorique, Université de Paris-Sud, 91405 Orsay, France, and Department of Chemistry, North Carolina State University, Raleigh, North Carolina 27695-8204

Similarity of the Electronic Properties of the Monophosphate Tungsten Bronzes

Enric Canadell,*† Myung-Hwan Whangbo,*† and Idris El-Idrissi Rachidi†

Received January 17, 1990

The electronic structures of the perovskite-type tungsten oxide (W–O) layers of the monophosphate tungsten bronzes (MPTB) were examined by performing tight-binding band calculations. Our study shows that all known MPTB phases have one- and two-dimensional metallic bands regardless of the difference in the thickness of their W–O layers and in their octahedral distortions. Concerning this dimensionality of the electronic properties, the bond valence sum analysis is found to give erroneous predictions. We examine the origin of this failure and also that of the remarkable similarity in the MPTB electronic structures.

The monophosphate tungsten bronzes (MPTB) contain perovskite-type layers made up of WO_6 octahedra, and these tungsten oxide (W–O) layers are interlinked by PO_4 tetrahedra.^{1,2} The thickness of these W–O layers increase with the number of WO_6 octahedra (per unit cell) used to form the layers. The MPTB phases have either pentagonal or hexagonal tunnels between the W–O layers, and they are called the $MPTB_p$ and $MPTB_h$ phases, respectively. The latter invariably occur with alkali-metal atoms Na or K, which reside in the hexagonal tunnels.² The third members of the $MPTB_p$ and $MPTB_h$ series, $(WO_3)_6(WO_3)_6(PO_2)_4$ and $A_x(WO_3)_6(WO_3)_6(PO_2)_4$ (A = alkali metal), are similar in structure to the Magnéli phases³ $\gamma-Mo_4O_{11}$ and $\eta-Mo_4O_{11}$, respectively, except that PO_4 tetrahedra are replaced by MoO_4 tetrahedra in the Magnéli phases. The latter exhibit resistivity anomalies,⁴ which originate from the electronic instability associated with the partially filled bands of their perovskite-type Mo–O layers.⁵ Since the MPTB phases possess isostructural W–O layers, they are also expected to show similar electronic instabilities. In fact, the third member of the $MPTB_p$ series, $(WO_3)_6(WO_3)_6(PO_2)_4$, exhibits resistivity anomalies⁶ strikingly similar to those of $NbSe_3$, a well-established charge-density-wave (CDW) material.⁷

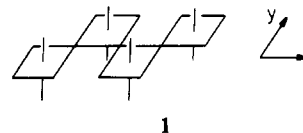
As will be discussed later, each perovskite-type W–O layer of the $MPTB_p$ series contains two d electrons per unit cell, regardless of its thickness. This electron counting is slightly modified in the $MPTB_h$ phases due to the alkali-metal atoms in their hexagonal channels. Thus, the MPTB phases provide a number of W–O layers with different average oxidation states of W. The crystal structures of the MPTB series reveal that the octahedral distortions in their W–O layers are not uniform even among those layers with a same thickness. In understanding the electronic properties of the MPTB phases, it is necessary to examine how their electronic structures are related to the crystal structure, the octahedral distortion, and the average oxidation state of W. In the present study, we investigate the electronic structures of all MPTB phases with known crystal structures by performing tight-binding band calculations⁸ based upon the extended Hückel method.⁹ The atomic parameters employed in the present study are taken from our previous work.¹⁰

Crystal Structure

Nearly all MPTB phases have two perovskite-type W–O layers per unit cell.^{1,2} Thus, the general formulas for the $MPTB_p$ phases can be written as $(WO_3)_p(WO_3)_q(PO_2)_4$, and those for the $MPTB_h$ phases as $A_x(WO_3)_p(WO_3)_q(PO_2)_4$ (A = Na, K). The indices p and q are even or odd integers, which are equal to the number of WO_6 octahedra (per unit cell) used to form the W–O layer.

Usually p and q are identical, thereby leading to the formulas $(WO_3)_{2m}(PO_2)_4$ and $A_x(WO_3)_{2m}(PO_2)_4$ (m = integer). However, they can be different as in the case of $(WO_3)_4(WO_3)_6(PO_2)_4$, which should be distinguished from $(WO_3)_5(WO_3)_5(PO_2)_4$.

The general structural patterns of the perovskite-type W–O layers may be described in terms of the W–O layer with $p = 4$. Diagram 1 shows a perspective view of the W_4O_{21} unit made up



- (1) (a) Giroult, J. P.; Goreaud, M.; Labbé, P.; Raveau, B. *Acta Crystallogr. Sect. B* **1981**, *B37*, 2139. (b) Labbé, P.; Goreaud, M.; Raveau, B. *Solid State Chem.* **1986**, *61*, 324. (c) Benmoussa, A.; Labbé, P.; Giroult, D.; Raveau, B. *J. Solid State Chem.* **1982**, *44*, 318. (d) Domengès, B.; Studer, F.; Raveau, B. *Mater. Res. Bull.* **1983**, *18*, 669. (e) Domengès, B.; Hervieu, M.; Raveau, B.; Tilley, R. J. D. *J. Solid State Chem.* **1984**, *54*, 10.
- (2) (a) Giroult, J. P.; Goreaud, M.; Labbé, P.; Raveau, B. *J. Solid State Chem.* **1982**, *44*, 407. (b) Benmoussa, A.; Giroult, D.; Labbé, P.; Raveau, B. *Acta Crystallogr., Sect. C* **1984**, *C40*, 573. (c) Domengès, B.; Goreaud, M.; Labbé, P.; Raveau, B. *J. Solid State Chem.* **1983**, *50*, 173. (d) Lamire, M.; Labbé, P.; Goreaud, M.; Raveau, B. *J. Solid State Chem.* **1987**, *66*, 64. (e) Benmoussa, A.; Giroult, D.; Raveau, B. *Rev. Chim. Min.* **1984**, *21*, 710.
- (3) (a) Ghedira, M.; Vincent, H.; Marezio, M.; Marcus, J.; Fourcadot, G. *J. Solid State Chem.* **1985**, *56*, 66. (b) Kihlberg, L. *Arkiv Kemi* **1963**, *21*, 365. (c) Magnéli, A. *Acta Chem. Scand.* **1948**, *2*, 861.
- (4) (a) Guyot, H.; Schlenker, C.; Fourcadot, G.; Konaté, K. *Solid State Commun.* **1985**, *54*, 909. (b) Sato, M.; Nakao, K.; Hoshino, S. *J. Phys. C* **1984**, *17*, L817. (c) Schlenker, C.; Parkin, S. S. P.; Guyot, H. *J. Magn. Magn. Mater.* **1986**, *54–57*, 1313. (d) Guyot, H.; Escribe-Filippini, C.; Fourcadot, G.; Konaté, K.; Schlenker, C. *J. Phys. C* **1983**, *16*, L1227.
- (5) Canadell, E.; Whangbo, M.-H.; Schlenker, C.; Escribe-Filippini, C. *Inorg. Chem.* **1989**, *28*, 1466.
- (6) Wang, E.; Greenblatt, M.; Rachidi, I. E.-I.; Canadell, E.; Whangbo, M.-H.; Vadlamannati, S. *Phys. Rev. B* **1989**, *39*, 12969.
- (7) (a) Monceau, P. In *Electronic Properties of Inorganic Quasi-One-Dimensional Compounds. Part II*. Monceau, P., Ed.; Reidel: Dordrecht, The Netherlands, 1985; p 139. (b) Haen, P.; Monceau, P.; Tissier, B.; Waysand, G.; Meerschaut, A.; Molinié, P.; Rouxel, J. In *Proceedings of the Fourteenth International Conference on Low Temperature Physics*; Krusius, M., Vuorio, M., Eds.; North Holland: New York, 1975. (c) Canadell, E.; Rachidi, I. E.-I.; Pouget, J. P.; Gressier, P.; Meerschaut, A.; Rouxel, J.; Jung, D.; Evain, M.; Whangbo, M.-H. *Inorg. Chem.* **1990**, *29*, 1401.
- (8) Whangbo, M.-H.; Hoffmann, R. *J. Am. Chem. Soc.* **1978**, *100*, 6093.
- (9) Hoffmann, R. *J. Chem. Phys.* **1963**, *39*, 1397. A modified Wolfsberg–Helmholz formula was used to calculate the off-diagonal H_{ij} values. See: Ammeter, J. H.; Burgi, H.-B.; Thibeault, J.; Hoffmann, R. *J. Am. Chem. Soc.* **1978**, *100*, 2686.
- (10) Wang, E.; Greenblatt, M.; Rachidi, I. E.-I.; Canadell, E.; Whangbo, M.-H. *Inorg. Chem.* **1989**, *28*, 2451.

* Université de Paris-Sud.

† North Carolina State University.